This is a peer-reviewed, author's accepted manuscript of the following conference output: Bayram, I. S. (2024).
Stochastic modelling of fast DC charging stations with shared power modules.
Paper presented at 2nd IEEE International Conference on Renewable Energies and Smart Technologies 2024, Pristina.

Stochastic Modelling of Fast DC Charging Stations with Shared Power Modules

I. Safak Bayram
Dept. of Electronic and Electrical Eng.
University of Strathclyde
Glasgow, United Kingdom
safak.bayram@strath.ac.uk

Kristian Sevdari
Dept. of Wind and Energy Systems
Technical University of Denmark-DTU
Roskilde, Denmark
krisse@dtu.dk

***Abstract*—Fast DC charging stations are becoming increasingly necessary for wider electric vehicle uptake. In standard DC chargers, each charging unit has its own charging power and cannot be shared with another electric vehicle. Depending on the electric vehicle type, the maximum DC charging power varies (e.g.50 kW for small sedans and $\geq$ 100 kW for SUVs) in parallel to battery chemistry and capacity. If the charger power is higher than the maximum charging capacity of an EV, then, charging resources are wasted for other vehicles which can accept high charging currents. On the other hand, recent advances in power electronics enable centralized inverters to supply power to multiple DC chargers and shift the load between them dynamically. To that end, we propose a stochastic model for a fast charging station in which the charging power modules are centrally located and electric vehicles are connected via external charging sockets. The charging station serves multi-class customers based on their charging power, random arrival and service durations. The system is modelled with a multi-rate Erlang loss system and a methodology to calculate the probability of meeting customer demand is presented. Case studies are presented to provide insights on how the station performs under varying station settings.**

I. Introduction

The widespread deployment of fast DC charging stations is a critical step in overcoming the challenge of charging electric vehicles (EV) and moving towards a deeper decarbonization of road transport. Fast DC charging is often characterized by a charging rate of more than 50 kW [1] and supports EV adoption to compete against petrol stations. Depending on the EV and charger type, these chargers can add up to 100 miles of range in less than half an hour. As a consequence, the number and coverage of fast DC charging stations have been increasing. In the United States, the number of DC charging stations reached 8200 distinct locations in 2024, one DC charging station for every 15 gas stations [2]. In the UK, nearly 20% of all chargers are fast DC (50+ kW rating) chargers [3], while similar patterns are observed in many other Western European countries and China [4].

Two key challenges related to deploying fast charging stations are grid constraints and the mismatch between the EV's maximum charging capability and the fast charger's capacity. For instance, consider a case where a Nissan Leaf is connected to a 100 kW charger (while it could only receive around 50 kW) and a Volkswagen ID.4 (with a maximum charging rate of 130 kW) is connected to a 50 kW socket. In this situation, the overall charging durations would increase due to the non-ideal usage of station resources, which negatively affects customer satisfaction. In addition, grid constraints typically enforce station capacity planning to be made following peak-hour spare capacity. This approach safeguards grid assets but limits EV charging during off-peak hours [5]. To address the aforementioned issues, the fast charging manufacturer, Kempower, has introduced a distributed approach to control the charging power at a site (see [6]. The power modules are centrally located in a cabinet that shares the charging power with different charging plugs (see satellite solution [6]).

This approach is gaining traction in the industry with other manufacturers, such as Eko Energetyka. The fast charging station is built from multiple identical power modules (e.g., each with a 25/40/50 kW rating [7]). The charging management software then assigns one or more power modules to each arriving customer to meet various customer demands shaped by the charging capabilities of individual EVs.

In this paper, we propose a stochastic model of such a fast DC charging station, which assigns multiple power sockets to different EV groups (or classes) which are differentiated based on charging capabilities (e.g., 50 kW vs. 100 kW, etc.) and arrival/departure patterns. The model is based on a multi-rate Erlang Loss system, and the goal is to compute the probability of meeting customer demand based on different station settings. The proposed methodology is rooted in multidimensional loss systems in teletraffic engineering, where the goal is to provide statistical quality of service guarantees to customers with different demand profiles.

Markov chain modelling of charging stations is increasing in the literature. In [8], a charging station composed of AC and DC chargers is modelled as a Markov chain, and an optimal pricing policy is introduced to maximize station profit. A similar modelling approach is presented in [9]. This work further includes on-site renewable generation and Vehicle to Grid capabilities. In several literature surveys (see [10] and [11]), EV charging station and load modeling is presented, which can provide wider technical explanation on the stochastic models used.

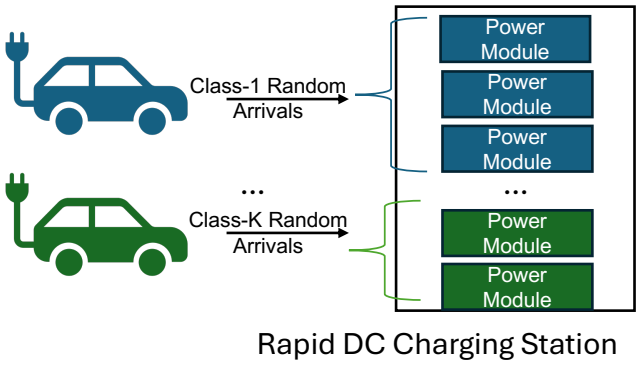

Fig. 1. Generic Station Model. There are K customer classes, each requesting different amount of charging resources.

II. Problem Formulation

A. System Description

We consider a fast DC charging station that serves multi-class EV demand categorized by the charging rate. AC / DC conversion is facilitated through P identical power modules (e.g., 25 kW each). The charging station serves K distinct customer cases determined by their arrival and departure processes, as well as their charging speeds. EVs in class $k \in 1, 2, ..., K$ use P_k number of power modules during charging. Furthermore, the number of charging modules is higher than each charging demand, that is, $P \gg P_k$, $\forall k$. In addition, it is assumed that the power conversion efficiency is close to 1, and the station capacity is denoted by C and has a unit in kW. Also, note the following linear relationship between the station capacity and the number of power modules: $C = P \times \text{capacity of each module}$. Therefore, C and P are used interchangeably in the rest of the paper.

Customer arrivals are assumed to be random and follow a Poisson process with rates λ_k for customer class k. Similarly, the charging process is assumed to follow Poisson with rates μ_k. It is noteworthy that the charging and arrival rates show, on average, the number of EV arrivals and charge completions in unit time. The charging demand (in kWh) for customer class k is denoted by D_k. Depending on the business model, D_k could be equal for each customer, as the business owner could enforce a rule (typically maximum charging demand) to minimize waiting times and reduce peak consumption. Note that Poisson arrival and departure processes are widely used in the literature to model fast charging station operations [12], [13]. Finally, it is assumed that there is no waiting space, and customers leave the station if all resources are in use upon their arrival. Therefore, the probability of not satisfying a customer's demand is a natural performance metric for this system. An overview of the station model is depicted in Fig. 1.

B. Markov Chain Model

The fast charging station described in the previous section is modeled as a multi-class loss system (also known as a multi-rate Erlang model [14]), which is used to model networks serving diverse customer classes with limited resources. As described previously, in this system, an EV is either admitted to the system or denied. Therefore, we are interested in computing such probabilities for varying station parameters such as the number of charging modules, arriving traffic density, and fast charging rates. To visualize the station model, a two-class Markov chain model is presented in Fig.2. In this model, the Markov chain states are represented by the tuple (i, j), which shows the number of EVs that the station can host from both customer classes. For instance, in State $(1, 1)$, there is one EV from each class. When the station is in this state, one of the following distinct events could occur:

- An EV finishes charging and leaves the station (with rate μ_1 for class-1 and with rate μ_2 for class-2).
- A new EV arrives at the station (with rate λ_1 for class-1 and with rate λ_2 for class-2).

Therefore, horizontal transitions represent the arrival and departure of class-1 EVs, and vertical transitions represent the arrival and departure of class-2 EVs. In both cases, the station's population can change by one EV at a time. The maximum number of EVs that can be charged simultaneously is represented by N_1 and N_2, which can be calculated by the equation:

$$N_1 = \left\lfloor \frac{P}{P_1} \right\rfloor, \qquad N_2 = \left\lfloor \frac{P}{P_2} \right\rfloor. \tag{1}$$

In Fig.2, states represented with N_1^* and N_2^* are residual states that could occur during the calculation of N_1 and N_2 in equation (1). The rightmost states in red font represent the cases where all station resources are in use. Therefore, computing the probabilities of being in red states will give the probability of "not serving" a customer, which is the main performance metric of the charging station.

C. Computation of Service Completion Probabilities

We aim to compute the service completion probabilities for a given station setting. It is noteworthy that the sum of the probability of "not serving" a customer (presented with red states in Fig.1) and the probability of service completion (SC) will always add up to one. Therefore, we will use these two terms interchangeably as the main performance metric.

To compute the probability of customer demand met, K independent time-reversible continuous-time Markov chains, representing each customer class, are analyzed. As previously discussed, the system state is defined by the number of EVs of each type, i.e., $\boldsymbol{N} \triangleq [N_1^P, N_2^P, \ldots, N_K^P]$ for a given station capacity P, and the state space is given by

$$\Omega \triangleq \{\boldsymbol{N} : \sum_{k=1}^{K} P_k N_k^{\infty} \leq P\}. \tag{2}$$

In the above state-space equation, the number of modules P is used instead of station capacity C to simplify the notation. It is noteworthy that the analysis starts by assuming there are infinitely many power modules available; hence, station states

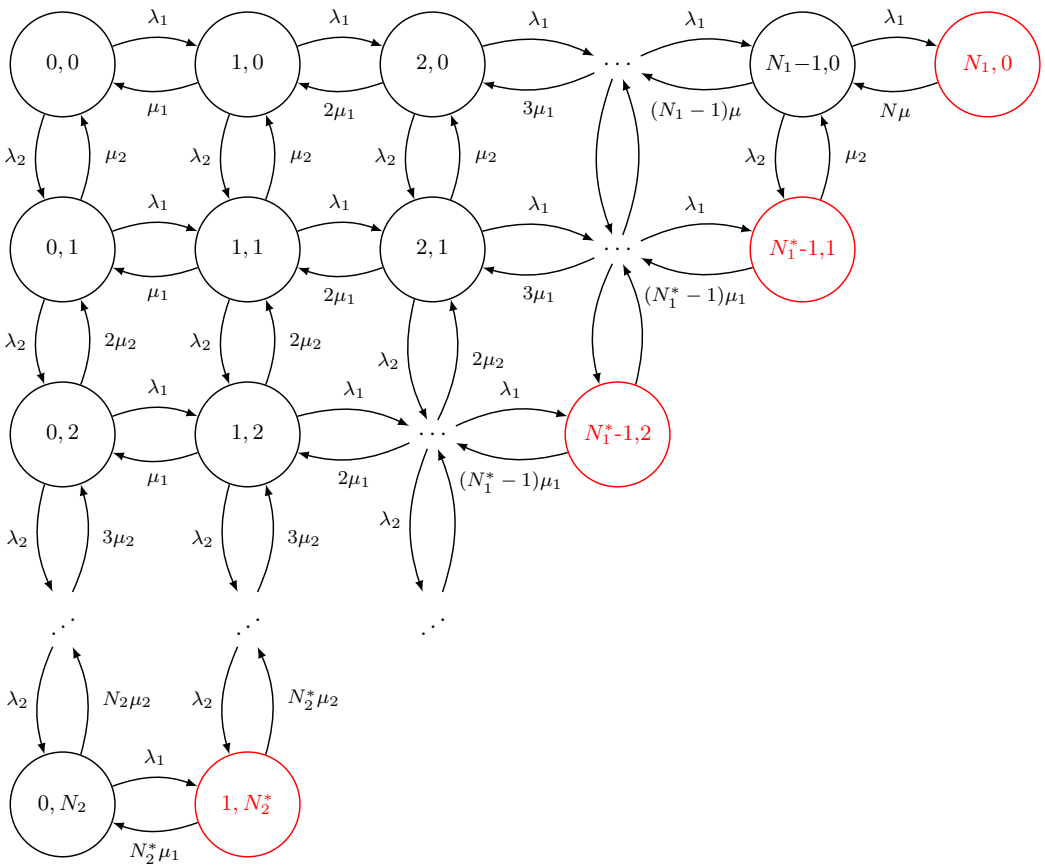

Fig. 2. Two class Markov chain model.

are represented by N^{∞}. Then the state probability distributions will be conditioned with respect to finite state capacity. The main reason for following this approach is that the literature presents closed-form expressions for the infinite capacity case, which can be used to derive the case with finite capacity. Note that due to the Poisson arrival process assumption, the mean and variance of N^{∞} become

$$\mathbb{E}\left[N_k^{\infty}\right] = \text{var}\left[N_k^{\infty}\right] = n_k = \frac{\lambda_k}{\mu_k} \tag{3}$$

Similar to (1), $\tilde{N}_k^P$ represent the highest number of EVs of type k that can be charged simultaneously. By ranking the charging rates in descending order $P_1 \geq P_2 \geq \cdots \geq P_K \geq 0$, the maximum number of EVs of each type that can be in the system has the following relation: $0 \leq \tilde{N}_1^P \leq \tilde{N}_2^P \leq \cdots \leq \tilde{N}_K^P$. Then the probability of being at an arbitrary state $\boldsymbol{N}$ can be written as [15]:

$$\overline{\pi}(\mathbf{N}) = \prod_{k=1}^{K} \frac{n_k^{N_k^{\infty}}}{N_k^{\infty}!} e^{-n_k} \ . \tag{4}$$

In the above equation, N_k^{∞} represents the number of EVs of class k that simultaneously request P_k power modules. By conditioning on a finite capacity, a generic system state $\boldsymbol{N}$ can be calculated as follows:

$$\pi(\boldsymbol{N}) = \frac{\overline{\pi}(\mathbf{N})}{\sum_{\tilde{N}\in\Omega} \overline{\pi}(\tilde{\mathbf{N}})}. \tag{5}$$

To calculate the probability of customer demand not met, the related system states for customer type k can be defined as:

$$\Psi_k = \{\boldsymbol{N} : P - P_k \ < \ \sum_{k=1}^{K} P_k N_k^C \ \leq \ P\} \tag{6}$$

Then, the probability of customer demand not met (NM) ($\mathbb{P}_{\mathbb{k}}{}^{NM}$) can be re-written as:

$$\mathbb{P}_{\mathbb{k}}{}^{NM}(\boldsymbol{n}, \boldsymbol{P}) = \sum_{s\in\Psi_k} \pi(s) = 1 - \sum_{s\notin\Psi_k} \pi(s) \ . \tag{7}$$

In (7), the second term denotes the probability that the station falls below $P - P_k$ (instead of P), and $\pi(s)$ represents the steady-state probability distribution. Furthermore, let us define the function $R(P, K)$ as:

$$R(P,K) \triangleq \sum_{\{\boldsymbol{N}:\, \boldsymbol{nN} \leq P\}} \prod_{k=1}^{K} \frac{n_k^{N_k}}{N_k!} \ , \tag{8}$$

Algorithm 1 Kaufman-Roberts Algorithm [16]

Set $\kappa(0) = 0$ and $\kappa(i) = 0$ for $i \in \mathbb{R}^-$
for i=1 to P **do**
  $\kappa(i) = \frac{1}{i} \sum_{k=1}^{K} P_k n_k (k - P_k)$
end for
Compute $R = \sum_{i=1}^{P} \kappa(i)$
for i=0 to P **do**
  $\alpha(i) = \frac{\kappa(i)}{R}$
end for
for k=1 to K **do**
  $\mathbb{P}_k(\boldsymbol{n}, \boldsymbol{P}) = \sum_{i=P-P_k+1}^{P} \alpha(i)$
end for

which is used to compute the probability of customer demand not met (NM) for each class as follows

$$\mathbb{P}_{\mathbb{k}}(\boldsymbol{n}, \boldsymbol{P}) = 1 - \frac{R(P - P_k, K)}{R(P, K)}. \tag{9}$$

Note that set $\{\boldsymbol{N} : \boldsymbol{nN} \leq P\}$ in (8) hosts all system states that correspond to zero outage events. Although (9) shows an explicit representation for $\mathbb{P}_{\mathbb{k}}$, actual computation could be computationally heavy. To that end, we follow the Kaufman-Roberts algorithm to solve individual probabilities for each customer class. Kaufman-Roberts algorithm is a recursion-based solution and its details are presented in Algorithm 1.

III. Results

This section presents two case studies to evaluate the system described in the previous section. The primary goal is to compute the percentage of customer demand that can be met under varying station parameters such as capacity (C or P) and customer demand (or arrival rate λ_k). The fast charging station comprises power modules with an individual capacity of 25 kW. In the first case study, the charging station capacity is $C = 250$kW, hence there are $P = 10$ modules integrated to serve the customer demand. For both case studies, it is assumed that there are two customer classes. In class 1, the fast charging rate is 50 kW ($P_1 = 2$). This class is chosen to mimic mainstream vehicles such as Nissan Leaf and Renault Zoe [17]. The fast charging rate in the second customer class is assumed to be 75 kW ($P_2 = 3$) to mimic EVs that can accept higher charging power. It is assumed that the charging station operator allows all customers to charge 25 kWh, therefore, $D_1 = D_2 = 25$ kWh. To that end, the charge rate for customer class 1 becomes $\mu_1 = 2$ as in one hour and on average two customers from this class can be charged. Similarly, the service rate for the class-2 customers becomes $\mu_2 = 3$.

The input parameters for the simulation are the arrival rates for each class (λ_1 and λ_2) which are varied from 0.25 EVs/hour (or one EV for every four hours) to 3 EVs/hour. Using Algorithm 1, the percentage of satisfied demand is evaluated for both customer classes. For ease of representation, let us denote the percentage of satisfied demand by $\overline{\mathbb{P}_k}$, which is equal to $1 - \mathbb{P}_k$. Fig. 3 shows the evaluation for Class-1 customers with 50 kW charging rate. It can be seen that under light traffic regime ($\lambda_1 = 0.25$ and $\lambda_2 = 0.25$), nearly 99.99% of the customer demand can be satisfied. At the other extreme when $\lambda_1 = \lambda_2 = 3$, only 87.25% of the demand can be met. This is mainly because the station utilization rate significantly increases and more customers are "blocked" and not admitted.

Fig. 4 shows the percentage of satisfied demand for class-2 customers. The pattern and the relationship between $\overline{\mathbb{P}_2}$ and arrival rates are similar to the previous case. However, since the charging rate is higher and each customer demands more charging power, the percentage of satisfied demand is lower than class-1 customers. For instance, when $\lambda_1 = \lambda_2 = 3$, $\overline{\mathbb{P}_2} = 0.7821$ and $\overline{\mathbb{P}_1} = 0.8725$. The results presented in Figs. 3 and 4 further show that a unit increase in Class-2 customer traffic has a higher impact on reducing $\overline{\mathbb{P}_1}$ and $\overline{\mathbb{P}_2}$. This is because Class-2 customers occupy more resources (75 kW) compared to Class-1 customers and station resources are utilized faster.

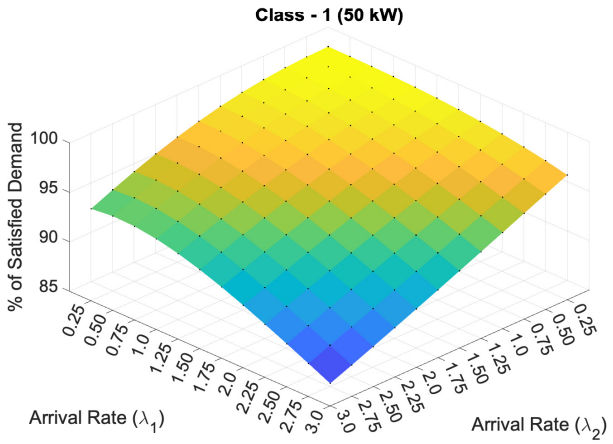

Fig. 3. Percentage of Class-1 EV demand met in a 250 kW fast charging.

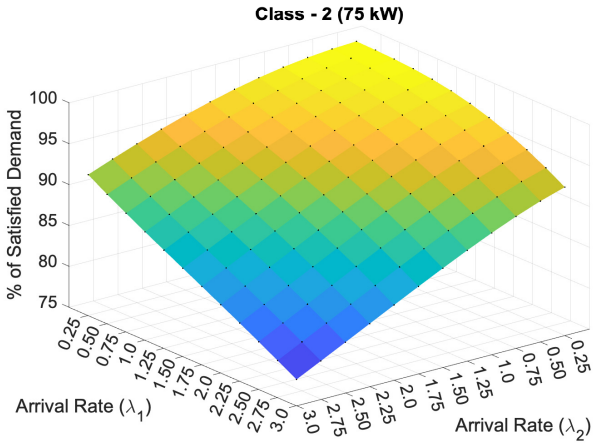

Fig. 4. Percentage of Class-2 EV demand met in a 250 kW fast charging

As a second case study, the station capacity is increased to $C = 500$ kW or $P = 20$. It can be seen from Figs. 5 and 6 that increasing station capacity significantly improves system performance. For both customer classes, the percentage of demand met increases to more than 99% for the high-traffic

case ($\lambda_1 = \lambda_2 = 3$). This result shows that station operators can adjust their station capacity to provide certain quality of service guarantees for their customers.

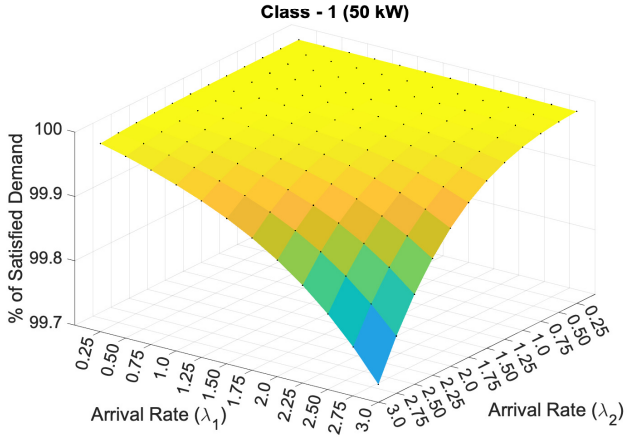

Fig. 5. Percentage of Class-1 EV demand met in a 500 kW fast charging

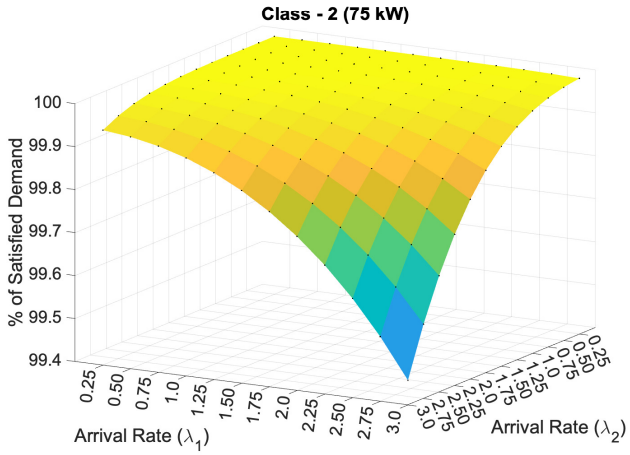

Fig. 6. Percentage of Class-2 EV demand met in a 500 kW fast charging

IV. Conclusion

In this paper, we proposed a stochastic model for a fast DC charging station in which power modules are centrally located and could be used by any of the physical chargers. The station is modeled as a multi-rate Erlang loss system with K distinct customer classes. Each customer class is characterized by their arrival and service rates, as well as charging demand. The station's performance is characterized by the probability of meeting customer demand. Then, we showed how to compute this probability based on different parameters using the Kaufman-Roberts algorithm. Case studies were presented to provide further insights on how to calculate station capacity to provide a certain quality of service to different customer classes.

As a future study, we will consider dynamic resource allocation to customers and assign lower charging rates to utilize the remaining available power. In addition, we will update our model for limited waiting space for facilities that allow 15-20 min waiting times.

Acknowledgement

The work of Kristian Sevdari was supported by the research project AHEAD (Horizon Europe grant no. 101160665).

References

[1] P. Franzese, D. D. Patel, A. A. S. Mohamed, D. Iannuzzi, B. Fahimi, M. Risso, and J. M. Miller, "Fast dc charging infrastructures for electric vehicles: Overview of technologies, standards, and challenges," *IEEE Transactions on Transportation Electrification*, vol. 9, no. 3, pp. 3780–3800, 2023.

[2] The US Now Has a Fast EV-Charging Station for Every 15 Gas Stations. https://www.bloomberg.com/news/articles/2024-04-18/the-us-now-has-a-fast-ev-charging-station-for-every-15-gas-stations. Online; accessed June 13, 2024.

[3] Electric vehicle charging device statistics: October 2023. https://www.gov.uk/government/statistics/electric-vehicle-charging-device-statistics-october-2023/electric-vehicle-charging-device-statistics-october-2023. Online; accessed June 13, 2024.

[4] Navigating Europe's EV Charging Expansion. https://statzon.com/insights/ev-charging-points-europe. Online; accessed June 13, 2024.

[5] L. Hunter, R. Sims, and S. Galloway, "Open data to accelerate the electric mobility revolution: Deploying journey electric vehicle chargers in rural scotland," *IEEE Power and Energy Magazine*, vol. 21, no. 6, pp. 56–67, 2023.

[6] Benefits of Choosing Dynamic Power for Public EV Charging Sites. https://kempower.com/dynamic-power-for-public-ev-charging-sites/. Online; accessed June 13, 2024.

[7] Electric Vehicle Power Module. https://en.sinexcel.com/evcharger/40kW.php. Online; accessed June 13, 2024.

[8] I. Zenginis, J. Vardakas, N. Zorba, and C. Verikoukis, "Performance evaluation of a multi-standard fast charging station for electric vehicles," *IEEE Transactions on Smart Grid*, vol. 9, no. 5, pp. 4480–4489, 2018.

[9] S. Esmailirad, A. Ghiasian, and A. Rabiee, "An extended m/m/k/k queueing model to analyze the profit of a multiservice electric vehicle charging station," *IEEE Transactions on Vehicular Technology*, vol. 70, no. 4, pp. 3007–3016, 2021.

[10] Y. Xiang, S. Hu, Y. Liu, X. Zhang, and J. Liu, "Electric vehicles in smart grid: a survey on charging load modelling," *IET Smart Grid*, vol. 2, no. 1, pp. 25–33, 2019.

[11] M.-O. Metais, O. Jouini, Y. Perez, J. Berrada, and E. Suomalainen, "Too much or not enough? planning electric vehicle charging infrastructure: A review of modeling options," *Renewable and Sustainable Energy Reviews*, vol. 153, p. 111719, 2022.

[12] I. S. Bayram, M. Devetsikiotis, and R. Jovanovic, "Optimal design of electric vehicle charging stations for commercial premises," *International Journal of Energy Research*, vol. 46, no. 8, pp. 10 040–10 051, 2022.

[13] L. Zhang and Y. Li, "Optimal management for parking-lot electric vehicle charging by two-stage approximate dynamic programming," *IEEE Transactions on Smart Grid*, vol. 8, no. 4, pp. 1722–1730, 2017.

[14] A. Nilssona, M. Perryb, A. Gershtc, and V. Iversend, "On multi-rate erlang-b computations," *Population*, vol. 2, p. b2, 1999.

[15] S. K. Bose, *An introduction to queueing systems*. Springer Science & Business Media, 2013.

[16] D. H. Tsang and K. W. Ross, "Algorithms to determine exact blocking probabilities for multirate tree networks," *IEEE transactions on communications*, vol. 38, no. 8, pp. 1266–1271, 1990.

[17] Electric Vehicle Database. https://ev-database.org/uk/. Online; accessed June 13, 2024.